Network Localized Granger Causality Inference: Performance Evaluation and Application to MEG Data

Behrad Soleimani[1,2], *Proloy Das*[1,2], *I.M. Dushyanthi Karunathilake*[1,2], *Stefanie E. Kuchinsky*[3], *Behtash Babadi*[1,2], *Jonathan Z. Simon*[1,2,4]

**behrad@umd.edu*

[1]Department of Electrical and Computer Engineering, [2]Institute for Systems Research, [3]Department of Speech and Hearing Sciences, [4]Department of Biology
University of Maryland, College Park, MD

Introduction

- Identifying causal relationships between different cortical areas for understanding mechanisms behind sensory processing
- Connectivity characterized by the temporal predictability of activity across brain regions via Granger causality (GC)
- Challenges with Magnetoencephalography (MEG) and Electroencephalography (EEG): the data are low-dimensional, noisy, and linearly-mixed versions of source activities
- Conventional methods (two-stage procedure):

- Drawbacks: bias propagation, spatial leakage

- Goal: *directly* localize GC influences without an intermediate source localization step
- Method: Network Localized Granger Causality (NLGC)
- Source dynamics as latent multivariate autoregressive model:

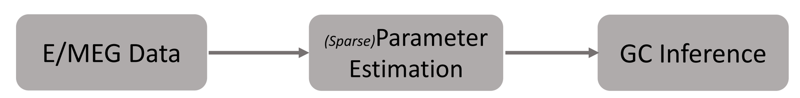

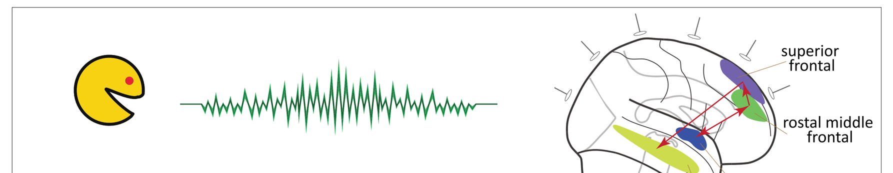

Fig. 1. Schematic depiction of connectivity during speech processing.

Model

- Observation model:

$$\mathbf{y}_t = \mathbf{C}\mathbf{x}_t + \mathbf{n}_t, \quad t = 1, 2, \cdots, T$$

$\mathbf{y}_t \in \mathbb{R}^M$ MEG observation, $\mathbf{C} \in \mathbb{R}^{M\times N}$ lead field matrix
$\mathbf{x}_t \in \mathbb{R}^N$ source activity, $\mathbf{n}_t \in \mathbb{R}^M$ measurement noise

- Source dynamic model (auto-regressive):

$$\mathbf{x}_t = \sum_{k=1}^{q} \mathbf{A}_k \mathbf{x}_{t-k} + \mathbf{w}_t, \quad t = 1, 2, \cdots, T$$

$\mathbf{A}_k \in \mathbb{R}^{N\times N}$ coefficient matrix, $\mathbf{w}_t \in \mathbb{R}^N$ noise process

- Distributional assumptions:
  - $\mathbf{n}_t \sim$ zero-mean Gaussian (known covariance)
  - $\mathbf{w}_t \sim$ zero-mean Gaussian, independent sources (unknown diagonal covariance $\mathbf{Q}$)

Granger Causality

- Consider link $(\tilde{i} \to i)$ with following models:

$$\text{Full: } \mathbf{x}_t^{(i)} = \sum_j \sum_k a_{i,j,k}\mathbf{x}_{t-k}^{(j)} + \mathbf{w}_t^{(i)}, \quad \mathbf{w}_t^{(i)} \sim \mathcal{N}(0, \sigma_i^2)$$

$$\text{Reduced: } \mathbf{x}_t^{(i)} = \sum_{j\neq\tilde{i}} \sum_k a'_{i,j,k}\mathbf{x}_{t-k}^{(j)} + \mathbf{w'}_t^{(i)}, \quad \mathbf{w'}_t^{(i)} \sim \mathcal{N}(0, \sigma_{i\setminus\tilde{i}}^2)$$

- Granger Causality (GC) measure:

$$\mathcal{F}_{(\tilde{i}\to i)} = \log\left(\frac{\sigma^2_{i\setminus\tilde{i}}}{\sigma_i^2}\right)$$ relative predictive variance explained

- $\mathcal{F}_{(\tilde{i}\to i)} \gg 0$: GC link exists.

Fig. 2. GC link $(\tilde{i} \to i)$ implies temporal predictability of source i by $\tilde{i}$.

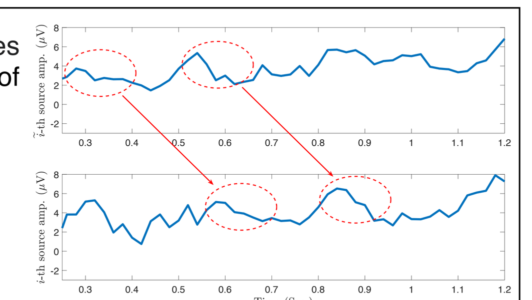

Parameter Estimation

- Objective: to estimate dynamic source model parameters

$$\boldsymbol{\theta} = (\mathbf{A}_k, k = 1, \cdots, q; \text{diag}(\mathbf{Q}))$$

- Challenge: source activities are unknown
- Solution: Expectation Maximization (EM)
- At the l-th iteration:

$$\text{E-step}: \; Q(\boldsymbol{\theta}|\widehat{\boldsymbol{\theta}}^{(l)}) = \mathrm{E}\left[\log p(\mathbf{x}_{1:T}, \mathbf{y}_{1:T}; \boldsymbol{\theta}) \middle| \mathbf{y}_{1:T}; \widehat{\boldsymbol{\theta}}^{(l)}\right]$$

$$\text{M-step}: \; \widehat{\boldsymbol{\theta}}^{(l+1)} = \underset{\boldsymbol{\theta}}{\text{argmax}} \left\{ Q(\boldsymbol{\theta}|\widehat{\boldsymbol{\theta}}^{(l)}) + R_{\ell_1}(\boldsymbol{\lambda}, \boldsymbol{\theta}) \right\}$$

- Continue until convergence
- E-step: Run fixed-interval smoother [1].
- ℓ_1-norm regularization is utilized at the M-step to mitigate the ill-posedness resulting from the low-dimensional measurements
- M-step: Solve via IRLS [2].
- Regularization parameter λ : two-fold cross-validation
- Reduced model: Perform the same EM-based parameter estimation for every source pair (link).

Statistical Inference Algorithm

- For link $(\tilde{i} \to i)$, the *debiased deviance* is

$$\mathcal{D}_{(\tilde{i}\mapsto i)} = 2\big(\ell_i(\widehat{\boldsymbol{\theta}}_i^F) - \ell_i(\widehat{\boldsymbol{\theta}}_i^R)\big) - B(\widehat{\boldsymbol{\theta}}_i^F, \widehat{\boldsymbol{\theta}}_i^R)$$

$\ell_i(\boldsymbol{\theta}_i)$ log-likelihood of the $i\text{-th}$ source
$\widehat{\boldsymbol{\theta}}_i^F, \widehat{\boldsymbol{\theta}}_i^R$ full and reduced parameter estimates
$B(.)$ bias term (see [3] for details)

- Two hypothesis

$H_{(\tilde{i}\mapsto i),0}: \; \boldsymbol{\theta}_i = \boldsymbol{\theta}_i^R$: there is no GC influence
$H_{(\tilde{i}\mapsto i),1}: \; \boldsymbol{\theta}_i = \boldsymbol{\theta}_i^F$: there is a GC influence

- Asymptotic distribution as $T \to \infty$ [4]:

$$[\mathcal{D}_{(\tilde{i}\to i)} | H_{(\tilde{i}\mapsto i),0}] \xrightarrow{d} \chi^2(q)$$

$$[\mathcal{D}_{(\tilde{i}\to i)} | H_{(\tilde{i}\mapsto i),1}] \xrightarrow{d} \chi^2(q, \nu_{(\tilde{i}\to i)})$$

- How to find non-centrality parameter [5]?

$$\widehat{\nu}_{(\tilde{i}\mapsto i)} = \max\left\{ \textstyle\sum_{n=1}^{N} \mathcal{D}^{(n)}_{(\tilde{i}\mapsto i)}/N - q, 0\right\}$$

$\mathcal{D}^{(n)}_{(\tilde{i}\to i)}$ is the $n\text{-th}$ sample of the deviance

- False discovery rate (FDR) control:
  - Reject null hypothesis at a confidence level α
  - Control FDR via BY procedure [6]
- Test strength characterization:
  - Calculate Youden's J-statistic for all links

$$J_{(\tilde{i}\to i)} = 1 - \alpha - F_{\chi^2(q, \widehat{\nu}_{(\tilde{i}\to i)})}(F^{-1}_{\chi^2(q)}(1-\alpha))$$

  - $J_{(\tilde{i}\to i)} \approx 1 \; (\approx 0)$ implies high (low) statistical confidence
  - The GC map $\boldsymbol{\Phi}$:

$$[\boldsymbol{\Phi}]_{i,\tilde{i}} = \begin{cases} \text{sign}\Big(\sum_{k=1}^{q} \widehat{a}_{i,\tilde{i},k}\Big) J_{(\tilde{i}\to i)}, & i \neq \tilde{i} \\ 0, & \text{otherwise} \end{cases}$$

  - Sign: excitation(+), inhibition(-)

Results: Synthetic Data

- Simulation setup:
  - 155 MEG sensors
  - Head model: 'ico-1' source space (84 ROIs)
  - Contribution of each ROI is summarized by the leading eigenvectors within the ROI (eigenmode)
  - Measurement noise: empty room data
  - 3000 time samples (3 segments)
  - 10 trials are generated to measure average hit rate and false alarm
  - Exact vs. relaxed localization (mis-localization to neighboring sources)
  - {2,4,…,20} active sources explaining 90% of total power
  - Two scenarios:

# of eigenmodes	Data generation	Estimation
Model mis-match	10	2
No model mis-match	2	2

  - 0 dB SNR
  - Source dynamics: VAR(3) process
  - FDR is controlled at 2%
  - Comparison with two-stage procedures (standard MNE and dSPM for the source localization stage [7])

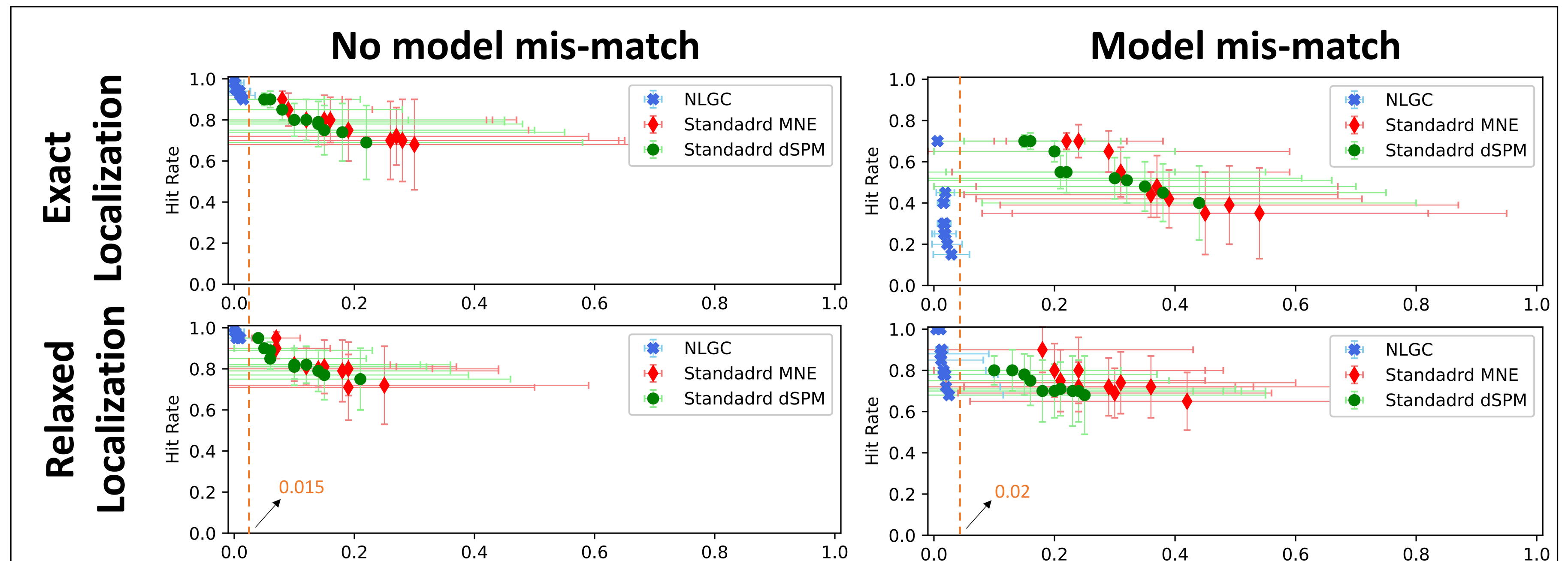

Fig. 3. Comparison of NLGC with two-stage procedures (standard MNE and dSPM) in two scenarios: with/without model mis-match. Overall, NLGC results in significantly less false alarms. In particular, at the worst case where there is model mis-match, NLGC achieves 2% false alarm (MNE: 43%, dSPM: 27%) and 69% hit rate (MNE: 69%, dSPM: 68%) which is substantially better than the two-stage procedures.

Results: Application to MEG Data

- Difficult listening experiment:
  - Task: 1-minute long speech segments from an audio book in two conditions:
    1) Clean speech: male/ female narration
    2) Mixed speech: two talker speech, male vs. female speaker
  - Mixed speech task: attend to pre-specified speaker
  - We analyzed the data from the first trials of these conditions
- Model specifications:
  - Band-pass between 0.1 – 4.5 Hz (Delta band) and downsample to 25 Hz
  - Head model: morph 'fsaverage' source space, Desican-Killiany atlas to identify 68 ROIs [8]
  - Analyzed ROIs (in both hemispheres):

Temporal lobe
'superiortemporal', 'middletemporal', 'transversetemporal'

Frontal lobe
'rostralmiddlefrontal', 'caudalmiddlefrontal', 'parsopercularis', 'parstriangularis'

- The measurement noise covariance: empty room recordings
- Contribution of each ROI is summarized by two eigenmodes
- 155 MEG sensors
- $q = 6$ is chosen (to fully capture the delta band)

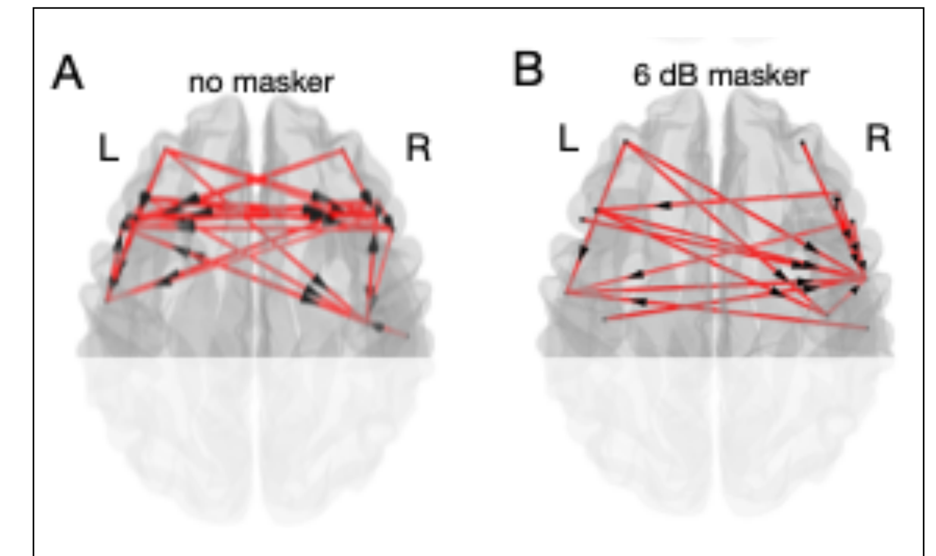

Fig. 4. NLGC estimates of neural connectivity for sites in the frontal and temporal lobes, during the last 40 s of each continuous speech listening trial, for either clean or masked speech (only significant links shown; arrows indicate direction of GC influence; N=4, FDR=1%). **A**. While listening to clean speech, about half (48%) of the significant causal links are frontal→frontal and about a third (32%) are top- down frontal→temporal (out of 31 significant links). B. In contrast, while listening to masked speech, almost two thirds (65%) of the 17 significant causal links are now top-down frontal→temporal, and only 12% are frontal→frontal (out of 17 significant links).

References

[1] B. D. Anderson and J. B. Moore, Optimal Filtering. Courier Corporation, 2012.

[2] D. Ba, B. Babadi, P. L. Purdon, and E. N. Brown, "Convergence and Stability of Iteratively Re-Weighted Least Squares algorithms," IEEE Transactions on Signal Processing, vol. 62, no. 1, pp. 183–195, 2013.

[3] B. Soleimani, P. Das, J. Kulasingham, J. Z. Simon and B. Babadi, "Granger Causal Inference from Indirect Low-Dimensional Measurements with Application to MEG Functional Connectivity Analysis," *2020 54th Annual Conference on Information Sciences and Systems (CISS)*, Princeton, NJ, USA, 2020, pp. 1-5.

[4] A. Sheikhattar, S. Miran, J. Liu, J. B. Fritz, S. A. Shamma, P. O. Kanold, and B. Babadi, "Extracting Neuronal Functional Network Dynamics via Adaptive Granger Causality Analysis," Proceedings of the National Academy of Sciences, vol. 115, no. 17, pp. E3869–E3878, 2018.

[5] K. L. Saxena and K. Alam,"Estimation of the Non Centrality Parameter of a Chi Squared Distribution," Ann. Stat., pp. 1012–1016, 1982.

[6] Y. Benjamini, D. Yekutieli et al., "The Control of the False Discovery Rate in Multiple Testing Under Dependency," Ann. Stat., vol. 29, no. 4, pp. 1165–1188, 2001

[7] Gramfort, Alexandre, et al. "MNE software for processing MEG and EEG data." Neuroimage, vol. 86, pp. 446–460, 2014.

[8] R. S. Desikan et al., "An Automated Labeling System for Subdividing the Human Cerebral Cortex on MRI Scans into Gyral based Regions of Interest," Neuroimage, vol. 31, no. 3, pp. 968–980, 2006.

Supported by NSF (SMA-1734892) and NIH (P01-AG055365, R01-DC014085).